Active Brownian Particles in 2d
Phase behavior and Dynamics

Leticia F. Cugliandolo

Sorbonne Université

Institut Universitaire de France

leticia@lpthe.jussieu.fr
www.lpthe.jussieu.fr/~leticia

Work in collaboration with

C. Caporusso, **G. Gonnella & I. Petrelli** (Bari, Italia)

P. Digregorio (Bari, Lausanne, Suisse & Barcelona, España)

A. Suma (Trieste, Italia, Philadelphia, USA & Bari, Italia)

D. Levis & I. Pagonabarraga (Barcelona, España & Lausanne, Suisse)

Newton Institute, 2023

Active Brownian disks

Focus on

- Full Pe - ϕ Phase diagram
- Mechanisms for phase transitions.
- Topological defects.
- Dynamics across phase transitions.
- Motility Induced Phase Separation.

- Influence of particle shape, *e.g.* disks *vs.* dumbbells.

Active Brownian Disks

(Overdamped) Langevin equations (the standard model)

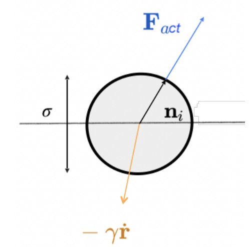

Active force $\mathbf{F}_{\rm act}$ along $\mathbf{n}_i = (\cos\theta_i, \sin\theta_i)$

$$m\ddot{\mathbf{r}}_i + \gamma\dot{\mathbf{r}}_i = F_{\rm act}\mathbf{n}_i - \nabla_i \sum_{j(\neq i)} U_{\rm Mie}(r_{ij}) + \boldsymbol{\xi}_i \ , \qquad \dot{\theta}_i = \eta_i \ ,$$

$\mathbf{r}_i$ position of ith particle & $r_{ij} = |\mathbf{r}_i - \mathbf{r}_j|$ inter-part distance,

$U_{\rm Mie}$ **short-ranged only repulsive** Mie potential, over-damped limit $m \ll \gamma$

$\boldsymbol{\xi}$ and η zero-mean Gaussian noises with

$\langle \xi_i^a(t)\, \xi_j^b(t')\rangle = 2\gamma k_B T \delta_{ij}^{ab}\delta(t-t')$ and $\langle \eta_i(t)\, \eta_j(t')\rangle = 2D_\theta \delta_{ij}\delta(t-t')$

The units of length, time and energy are given by σ, $\tau_p = D_\theta^{-1}$ and ε

$D_\theta = 3k_BT/(\gamma\sigma^2)$ controls persistence, $\gamma/m = 10$ and $k_BT = 0.05$

Péclet number Pe = $F_{\rm act}\sigma/(k_BT)$ measures activity and $\phi = \pi\sigma^2 N/(4S)$

Phase Diagram

Solid, hexatic, liquid, co-existence and MIPS

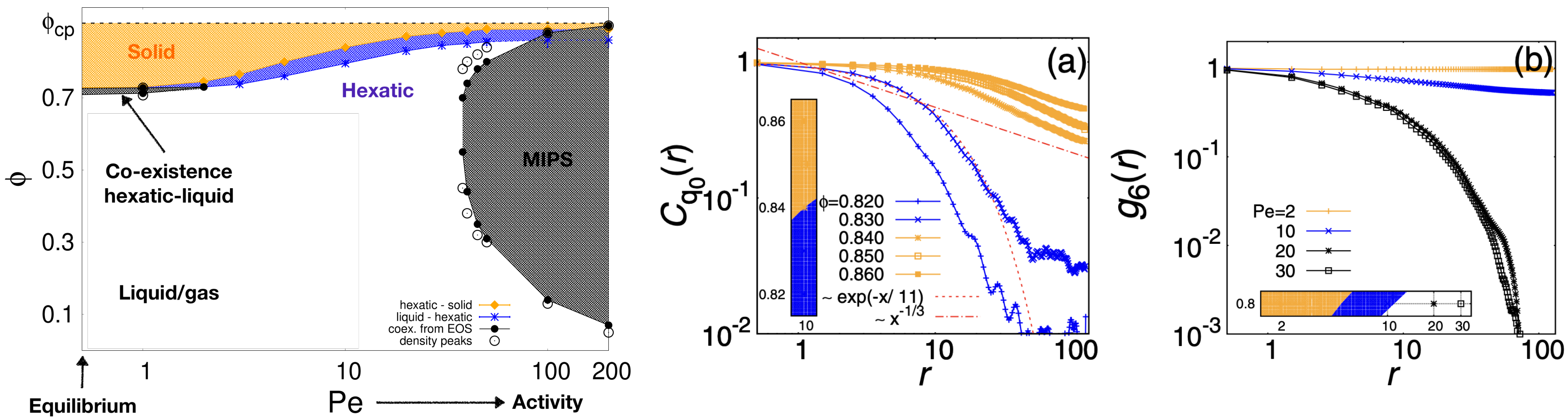

First order **liquid** - **hexatic** transition & co-existence at low Pe from

Pressure $P(\phi, \text{Pe})$ (EoS)

Distributions of local densities ϕ_i and local hexatic order parameters $|\psi_{6i}|$

Phases characterized by

Translational correlations $C_{q_0}(r)$ & orientational order correlations $g_6(r)$

Digregorio, Levis, Suma, LFC, Gonnella & Pagonabarraga, PRL 121, 098003 (2018)

Phase Diagram

Solid, hexatic, liquid, co-existence and MIPS

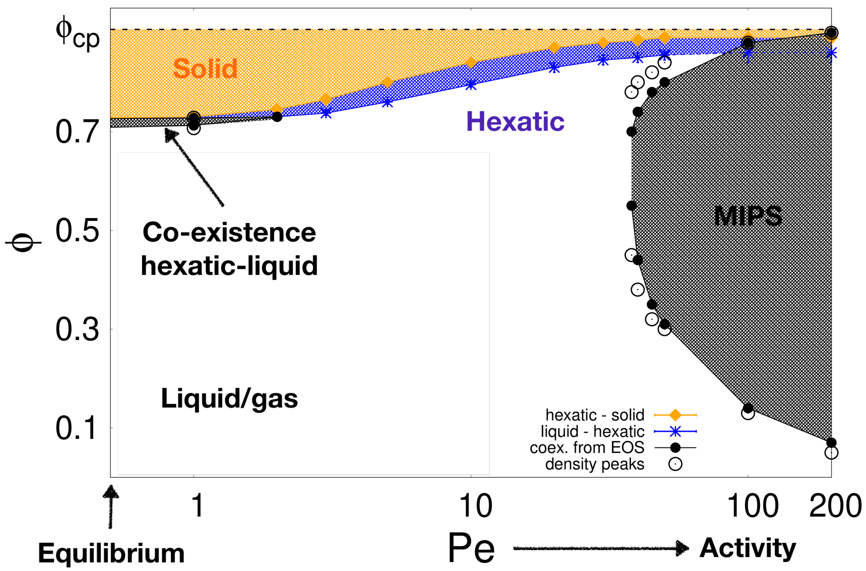

KT-HNY **solid-hexatic**

- universal KT-HNY dislocation unbinding

1st order **hexatic-liquid** close to Pe = 0

Breakdown of KT-HNY picture

- disclinations appear with the **liquid**

All along melting

- **percolation** of defect clusters

Defect identification, unbinding, & their densities

Digregorio, Levis, LFC, Gonnella & Pagonabarraga, Soft Matter 18, 566 (2022)

Mechanisms

Unbinding of defects ?

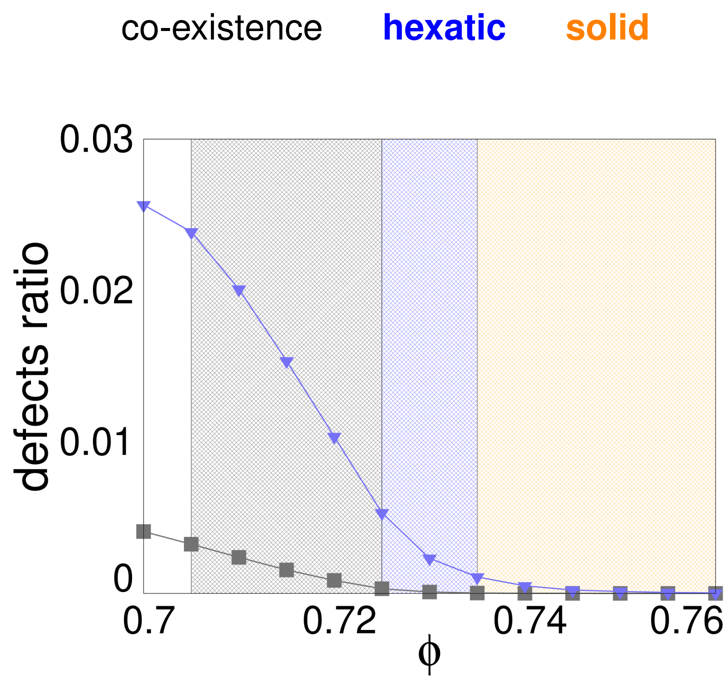

5 & 7 neighbors

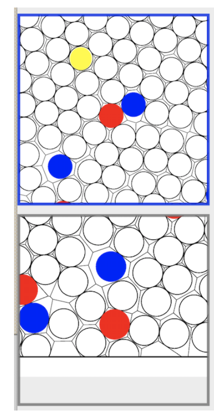

Dislocations ▼ unbind at the **solid** - **hexatic** transition as in BKT-HNY theory

$$\rho_{dislocations} \sim a \ \exp\left[-b\left(\frac{\phi_c}{\phi_c-\phi}\right)^{\nu}\right] \qquad \nu \sim 0.37$$

Disclinations ■ unbind when the **liquid** appears in the co-existence region

Digregorio et al. Soft Matter 18, 566 (22) ; experiments Han, Ha, Alsayed & Yodh, PRE 77, 041406 (08)

Defect clusters

At the hexatic - liquid transition (at all Pe)

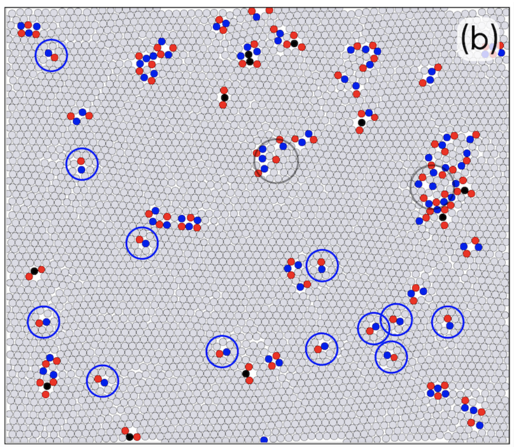

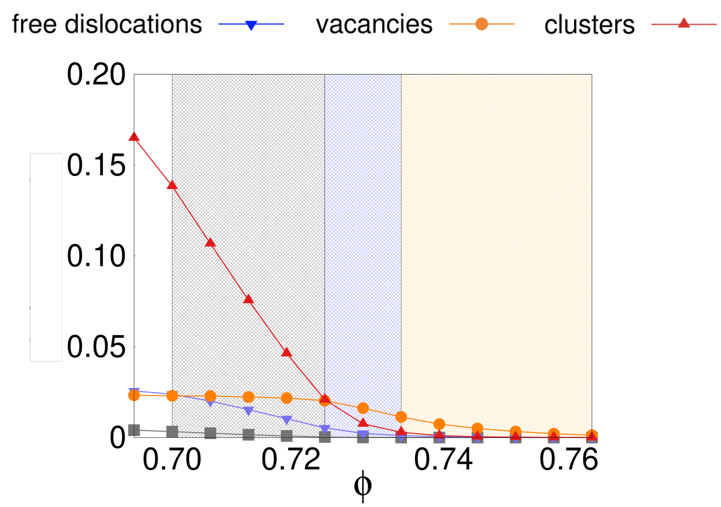

Very few disclinations, and always very close to other defects, **not free**

As soon as the liquid appears in co-existence, **many more defects in clusters**

Clusters percolate at (a bit ‘below’) the **hexatic**-**liquid** transition at all Pe with critical properties $\tau \sim 2.05$ & $d_f \sim 1.9$

Digregorio et al. Soft Matter 18, 566 (2022) ; also Qi, Gantapara & Dijkstra Soft Matter 10, 5419 (2014)

Active Brownian disks

Phase diagram with solid, hexatic, liquid, co-existence and MIPS

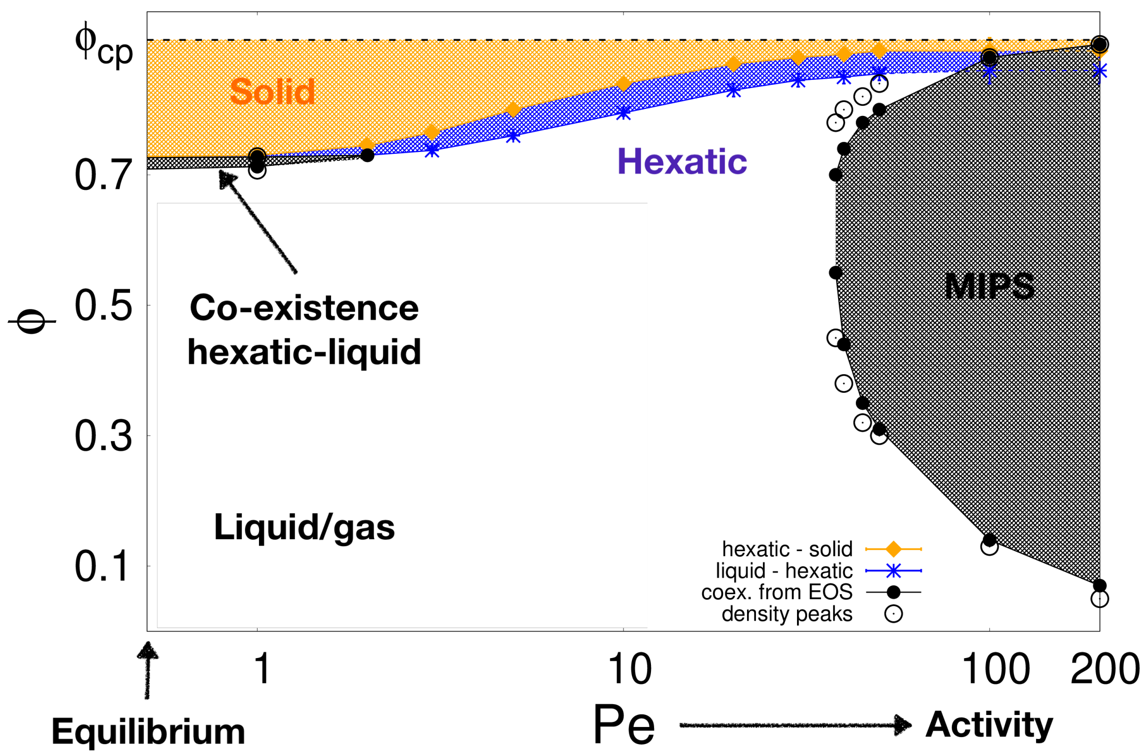

Motility induced

phase separation (MIPS)

gas & dense

Cates & Tailleur

Ann. Rev. CM 6, 219 (2015)

Farage, Krinninger & Brader

PRE 91, 042310 (2015)

Pressure $P(\phi, \mathrm{Pe})$ (EOS), correlations $C_{q_0}(r)$, $g_6(r)$, and distributions of ϕ_i, $|\psi_{6i}|$

Digregorio, Levis, Suma, LFC, Gonnella & Pagonabarraga, PRL 121, 098003 (2018)

MIPS

Highlights

— Growth of dense phase $R(t)$

— Growth of the hexatic order $R_H(t)$

— Density of bubbles $n(R_B, t)$

— Diffusion of clusters, $\Delta^2(M; t, t_0) \Rightarrow D(M, \mathrm{Pe})$

— Geometry of clusters, M_k vs. R_{g_k} $\Rightarrow$ fractality d_f

— **Beyond Ostwald ripening**, what is $R(t) \sim t^{1/3}$ due to ?

Growth of the dense phase

Scaling of the structure factor and growth regimes

Different Pe

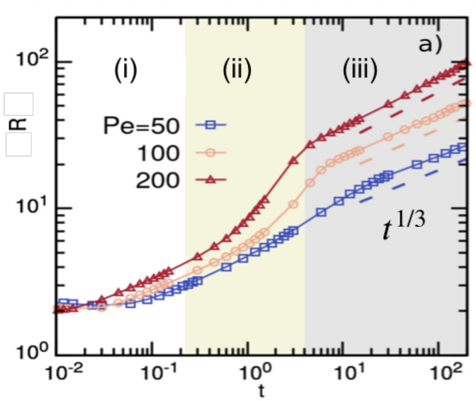

I peak:
system average
size

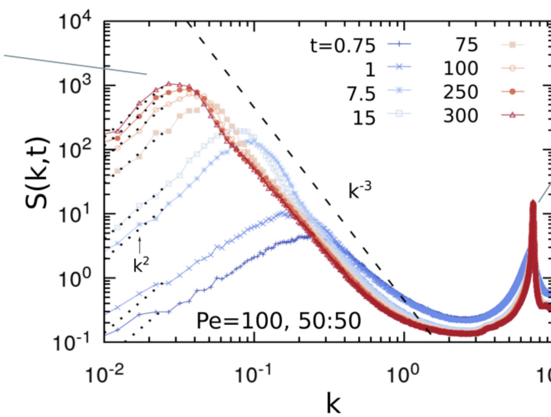

II peak:
particles' packing

$$S(\mathbf{k},t) = \sum_{i=1}^{N} e^{i\mathbf{k}(\mathbf{r}_i - \mathbf{r}_j)}$$

related to Fourier transform of
the pair correlation function

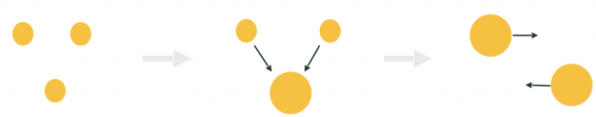

(i) nucleation (ii) condensation (iii) scaling

$$S(k,t) \sim R(t)^d\, f(kR(t))$$

$$R(t) \sim t^{1/3}$$

In the **scaling regime** $t^{1/3}$ like in **Lifshitz-Slyozov-Wagner**, scalar phase separation

Ostwald ripening small cluster evaporate and large ones capture gas particles

Redner et al, PRL 110, 055701 (13), Stenhammar et al, Soft Matter 10, 1489 (14)

but is it just that ?

Growth of the dense phase

Focus on the clusters

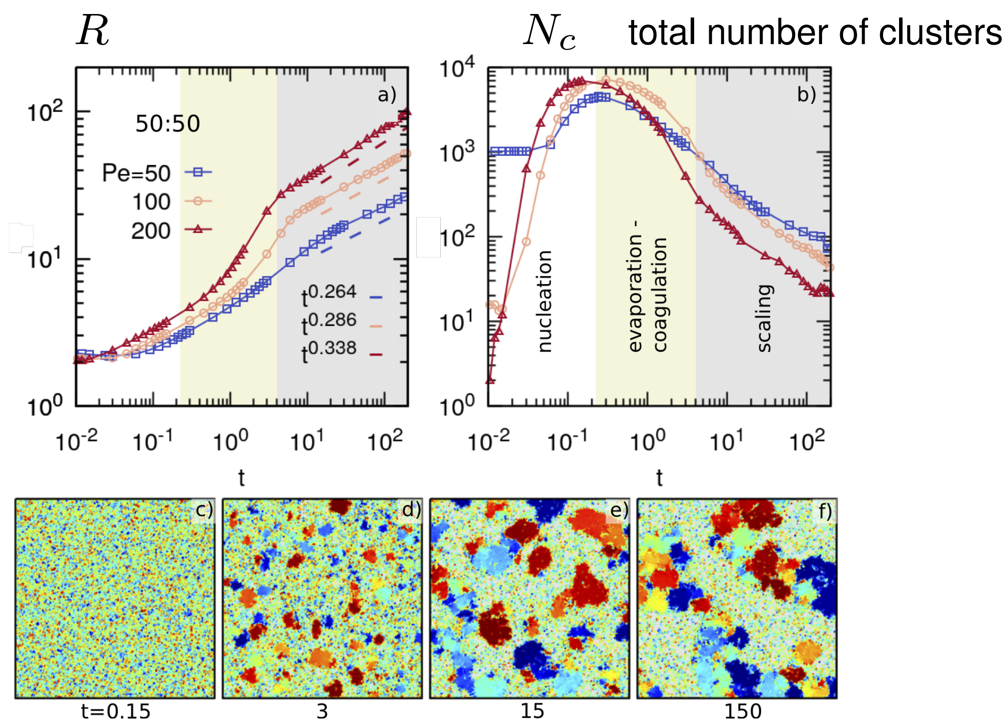

Nucleation Evap/coag Scaling

Beyond the averaged scaling regime **structure & dynamics**

Caporusso, Digregorio, Levis, LFC & Gonnella, PRL 125, 178004 (2020)

Caporusso, LFC, Digregorio, Gonnella, Levis & Suma, arXiv:2211.12361

The coloured patches

Local hexatic order parameter video

Orientational order

Local hexatic order parameter

$$\psi_{6j} = \frac{1}{nn_j} \sum_{k=1}^{nn_j} e^{i6\theta_{jk}}$$

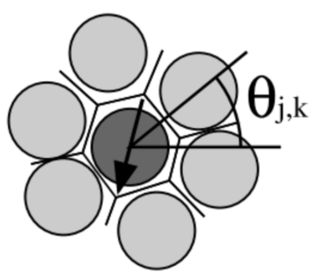

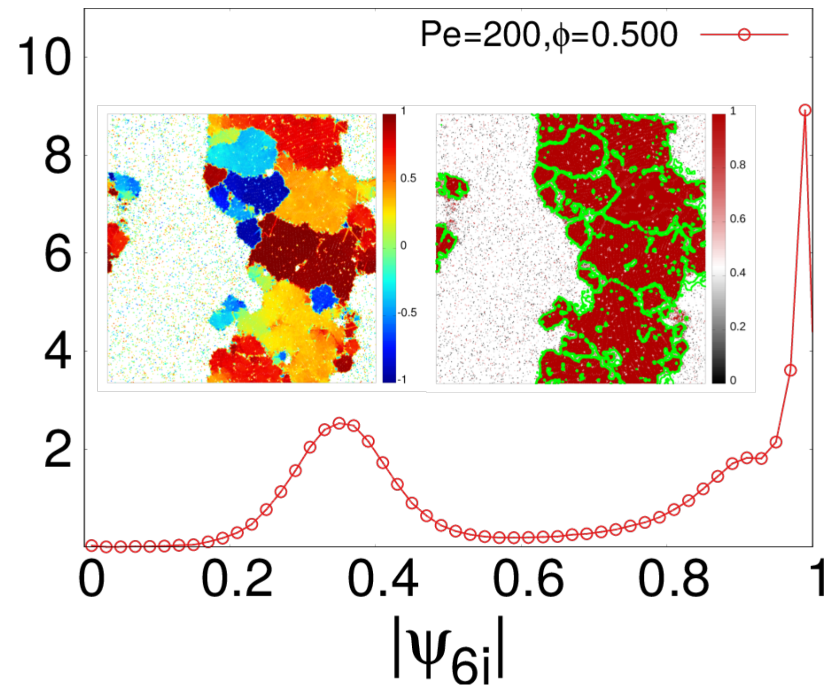

gas dense

Local hexatic order

Regimes

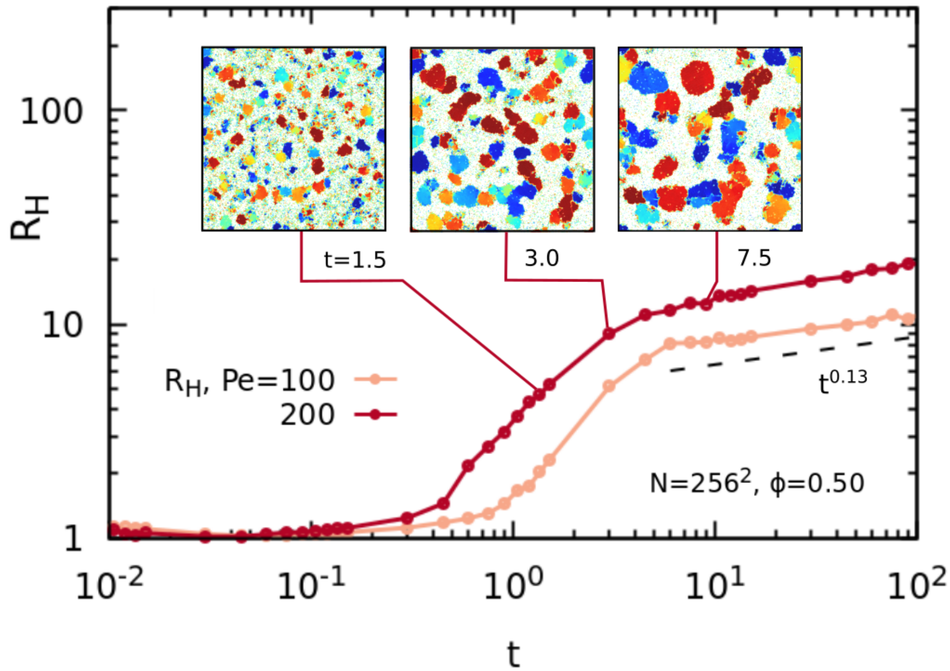

Full hexatically ordered small clusters

Larger clusters with several orientational order within

$R_H \sim t^{0.13}$ in the scaling regime and $R_H \to R_H^s \ll L$

Similar to pattern formation, e.g. **Vega, Harrison, Angelescu, Trawick, Huse, Chaikin & Register, PRE 71 061803 (2005)**

The growth process:

1. Is it like the one undergone by a system of **passive attractive particles**?

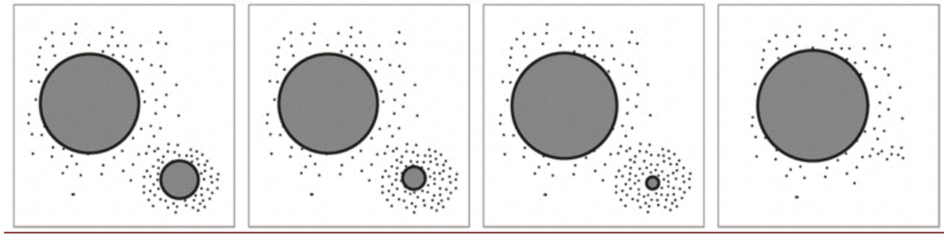

Ostwald ripening

2. Other are there other **mechanisms** at work?

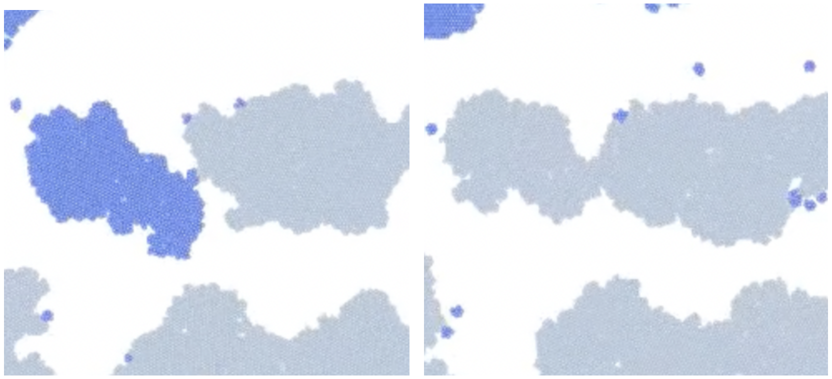

Cluster-cluster aggregation

Dense clusters

Instantaneous configurations (DBSCAN)

Passive

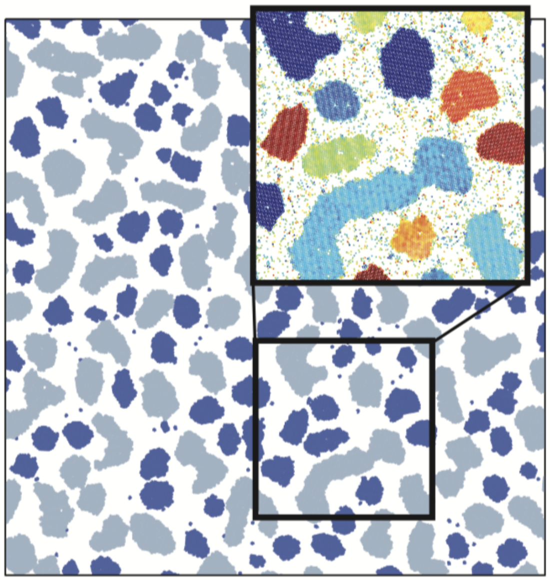

Active

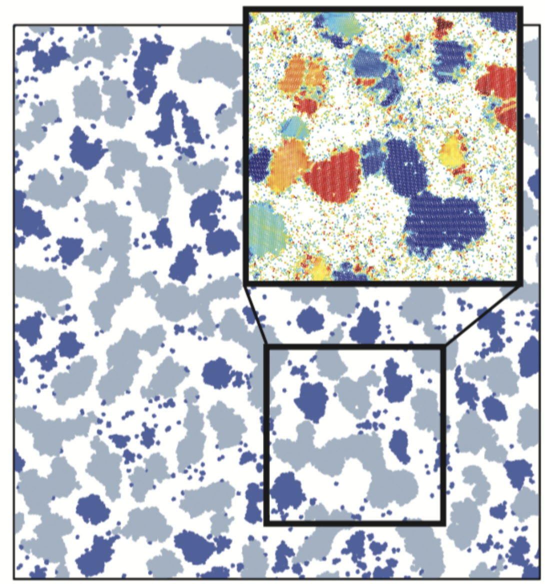

The Mie potential is not truncated in the passive case $\Rightarrow$ attractive

Parameters are such that $R(t)$ is the same

Colors in the zoomed box indicate orientational order

Caporusso, LFC, Digregorio, Gonnella, Levis & Suma, arXiv:2211.12361

Dense clusters

Visual facts about the instantaneous configurations

Similarities

- Large variety of shapes and sizes (masses)

  Co-existence of

  small regular (**dark blue**) and large elongated (**gray**) clusters

Differences

- Rougher interfaces in active
- Homogeneous (passive) vs. heterogeneous (active) orientational order within the clusters

Cluster dynamics

Tracking of individual cluster motion - video

Active

Passive

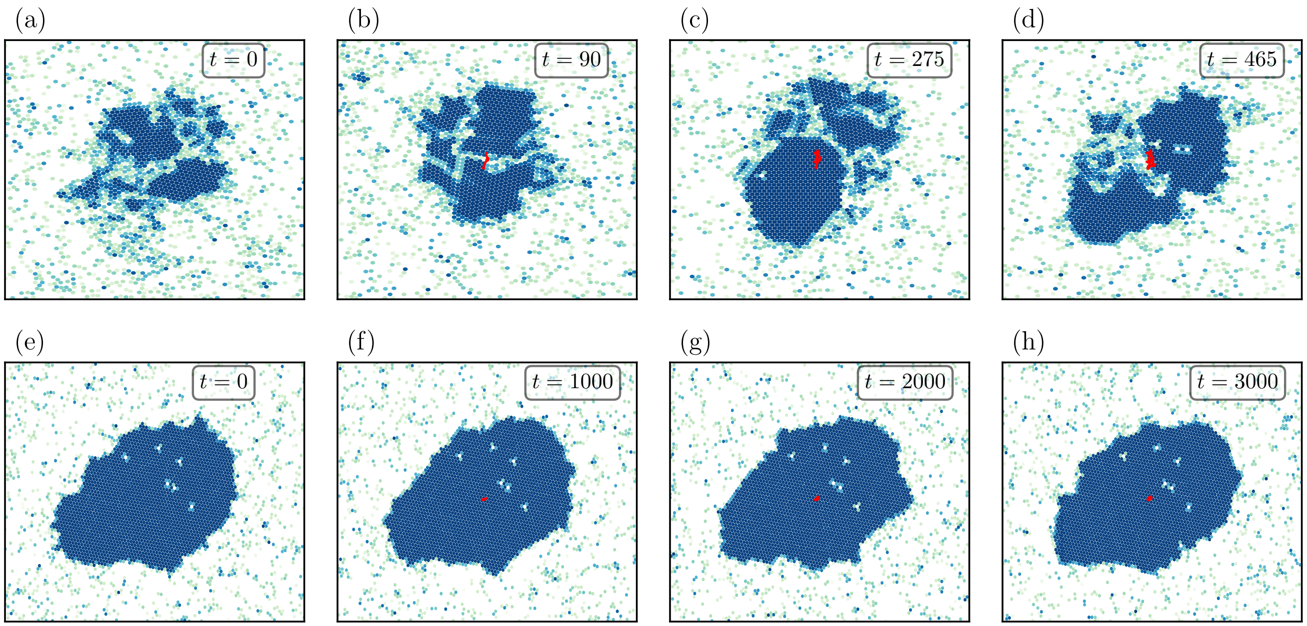

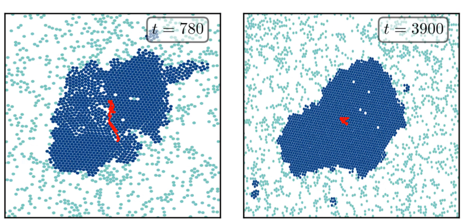

In **red** the center of mass trajectory

Active is much faster than passive

Dense clusters

Visual facts about the cluster dynamics

In both cases, **Ostwald ripening** features

- small clusters evaporate
- gas particles attach to large clusters

In the **active system**

- clusters displace much more & sometimes aggregate
- they also break & recombine

like in **diffusion limited cluster-cluster aggregation**

Dense clusters

Averaged mass $\overline{M} \equiv N_c^{-1}(t) \sum_{\alpha=1}^{N_c(t)} M_\alpha(t) \sim t^{2/3}$

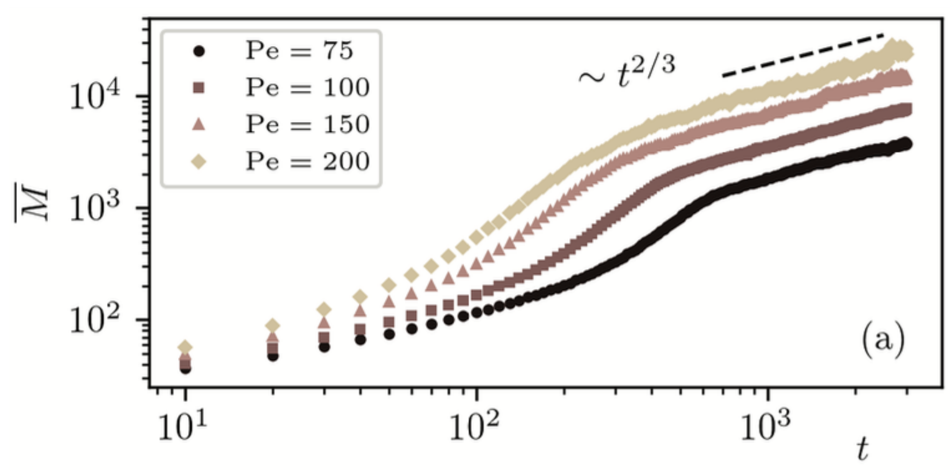

Same three regimes as in R from the structure factor

Clusters' dynamics origin ?

Active cluster evolution

Mean Square Displacement

Average over all clusters | **Cluster mass dependence**

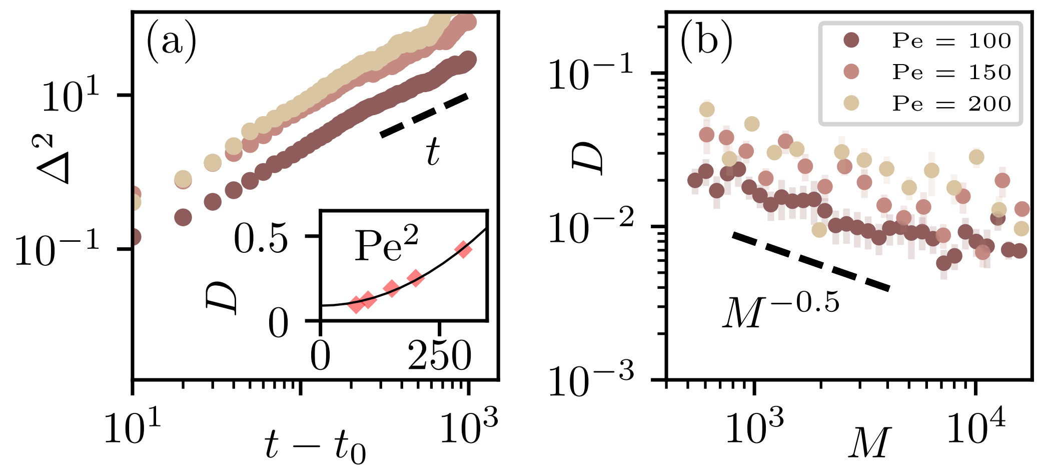

$$\Delta_k^2(t, t_0) = [\mathbf{r}_{\text{c.o.m.}}^{(k)}(t) - \mathbf{r}_{\text{c.o.m.}}^{(k)}(t_0)]^2 \sim 2d\, D(M_k, \mathrm{Pe})\, (t - t_0)$$

A sum of random forces yields $D \sim M^{-1}$

Passive tracer in a dilute active bath $D \sim R^{-1} \sim M^{-1/2}$ Solon & Horowitz (22)

Passive & very heavy isolated active clusters behave as $D \sim M^{-1}$

Geometry

Scatter plots: small regular – large fractal

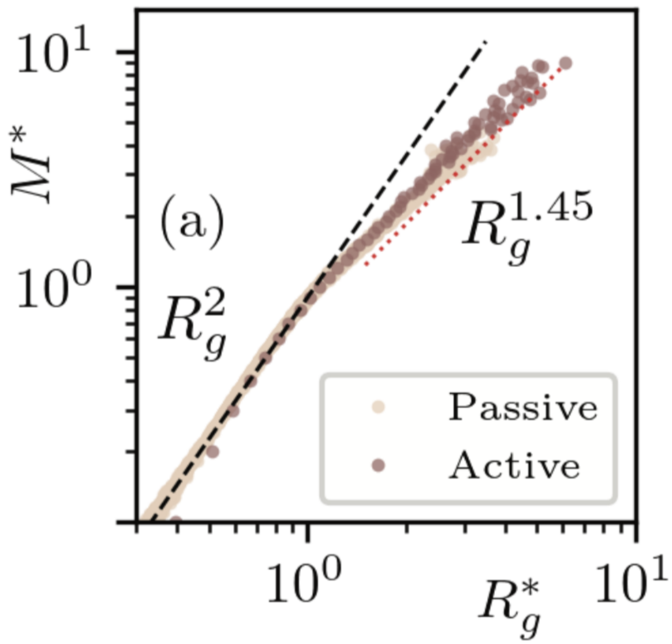

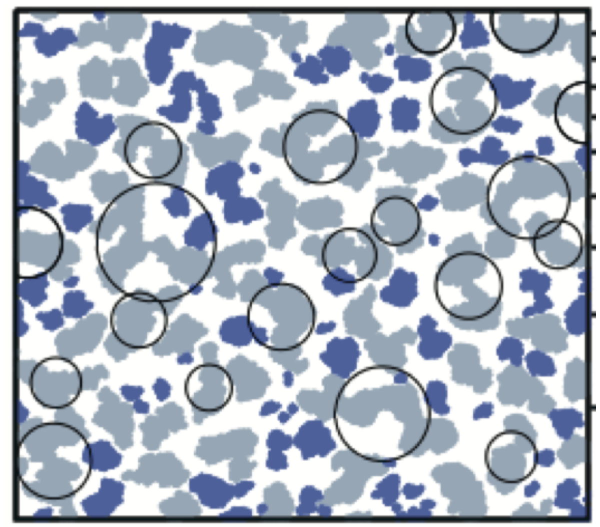

Cluster mass $M^*(t) = \dfrac{M_k(t)}{\overline{M}(t)}$ Gyration radius $R_g^*(t) = \dfrac{R_{g\,k}(t)}{\overline{R_g}(t)}$

Data sampled in the scaling regime $t = 10^3 - 10^5$ every 10^3 time steps

$\overline{M}(t) = \dfrac{1}{N_c(t)} \sum_{k=1}^{N_c(t)} M_k(t)$ and $N_c(t)$ the total number of clusters at time t

Cluster-cluster aggregation

Extended Smoluchowski argument

From $\overline{R}_g \sim t^{1/z}$ and using $D(M) \sim M^{-\alpha}$

Smoluchowski eq. $\Rightarrow z = d_f(1+\alpha) - (d - d_w)$

Regular clusters $M < \overline{M}$

$d_f = d = d_w = 2$

$\alpha = 0.5$

$z = 2(1+0.5) = 3$

Fractal clusters $M > \overline{M}$

$d_f = 1.45, d = 2$ and $d_w \sim 2$

$\alpha = 0.5$ in the bulk

$z = 1.45(1+0.5) = 2.18 < 3$

Reviews on the application of fractals to colloidal aggregation

R. Jullien, Croatia Chemica Acta 65, 215 (1992) P. Meakin, Physica Scripta 46, 295 (1992)

Regular vs fractal clusters

Radius of gyration and number

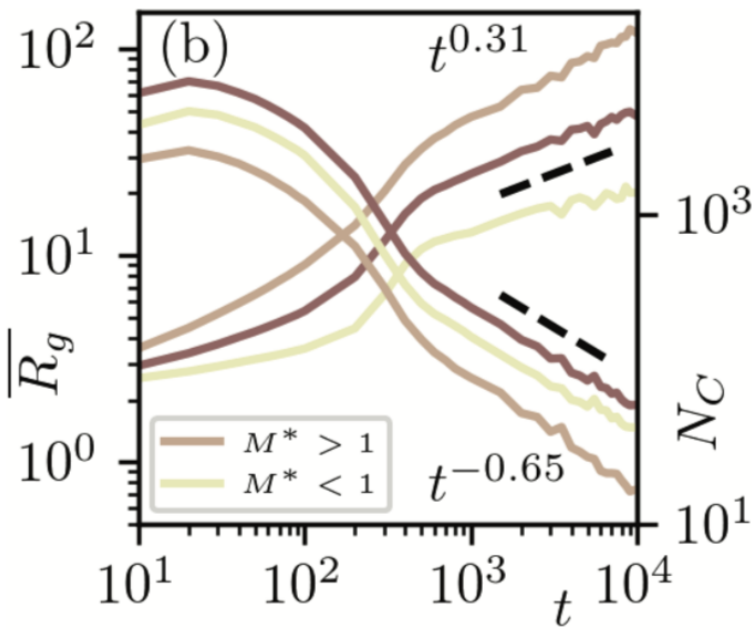

regular $z \gtrsim 3$ | fractal $z < 3$ | average $z = 1/0.31 \sim 3$

More Dominate | Less | All

Results I

We established the full phase diagram of ABPs

solid, **hexatic**, **liquid** & **MIPS**

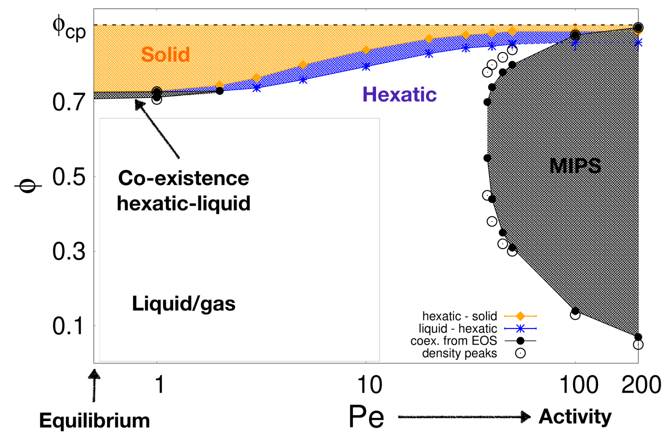

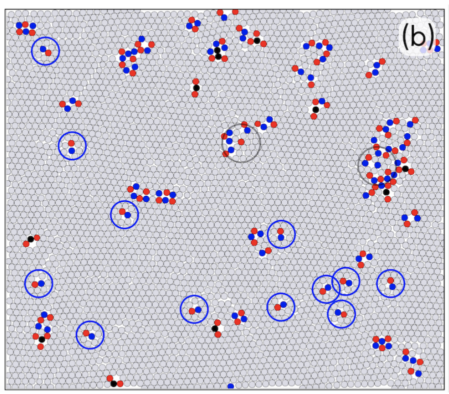

We clarified the role played by point-like (**dislocations** & **disclinations**) and **clustered** defects in passive & active $2d$ models.

In **MIPS**

Micro *vs.* macro : hexatic patches & bubbles

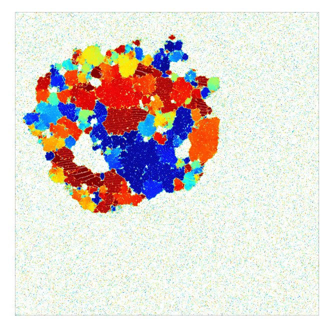

Results II

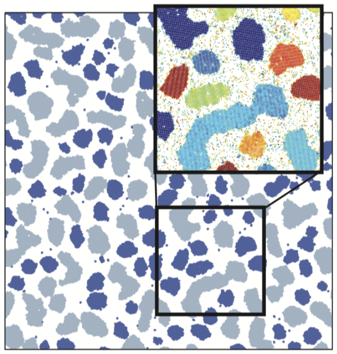

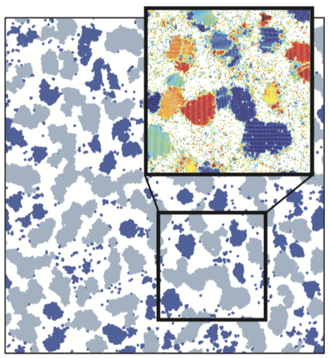

Difference between

Passive

Active

growth

Ostwald ripening & cluster-cluster aggregation in active case
cluster-cluster aggregation almost not present in passive

Co-existence of regular and fractal clusters

Heterogeneous orientational order in large active clusters

Beyond disks

Phase diagrams & plenty of interesting facts

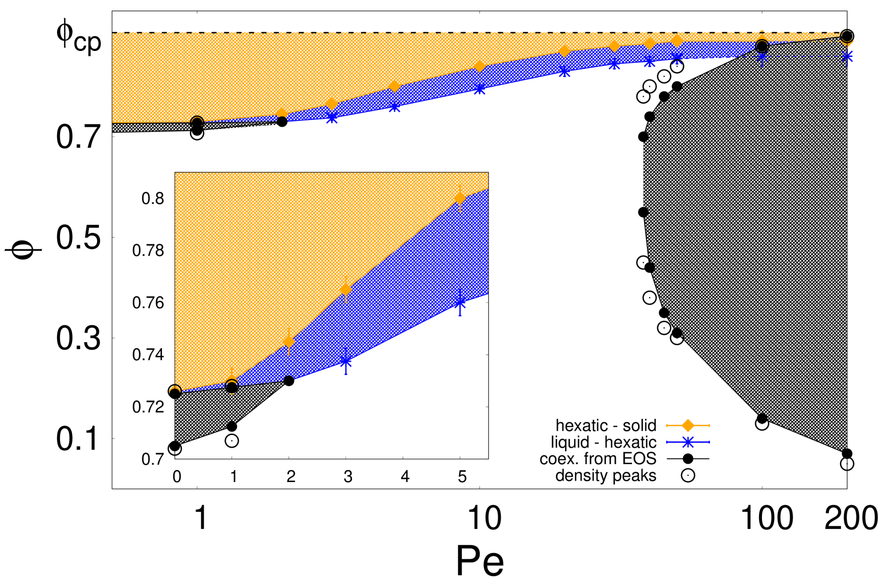

Disks

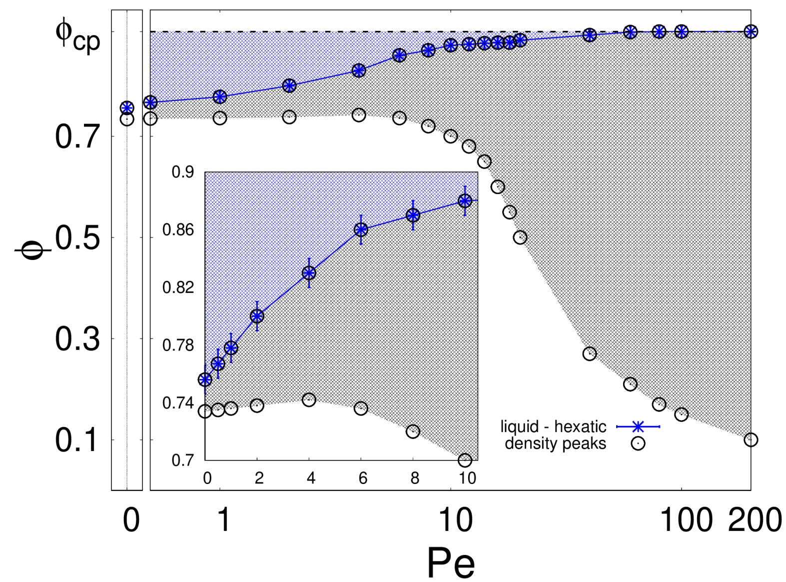

Dumbbells

Cluster mass distribution

Active system

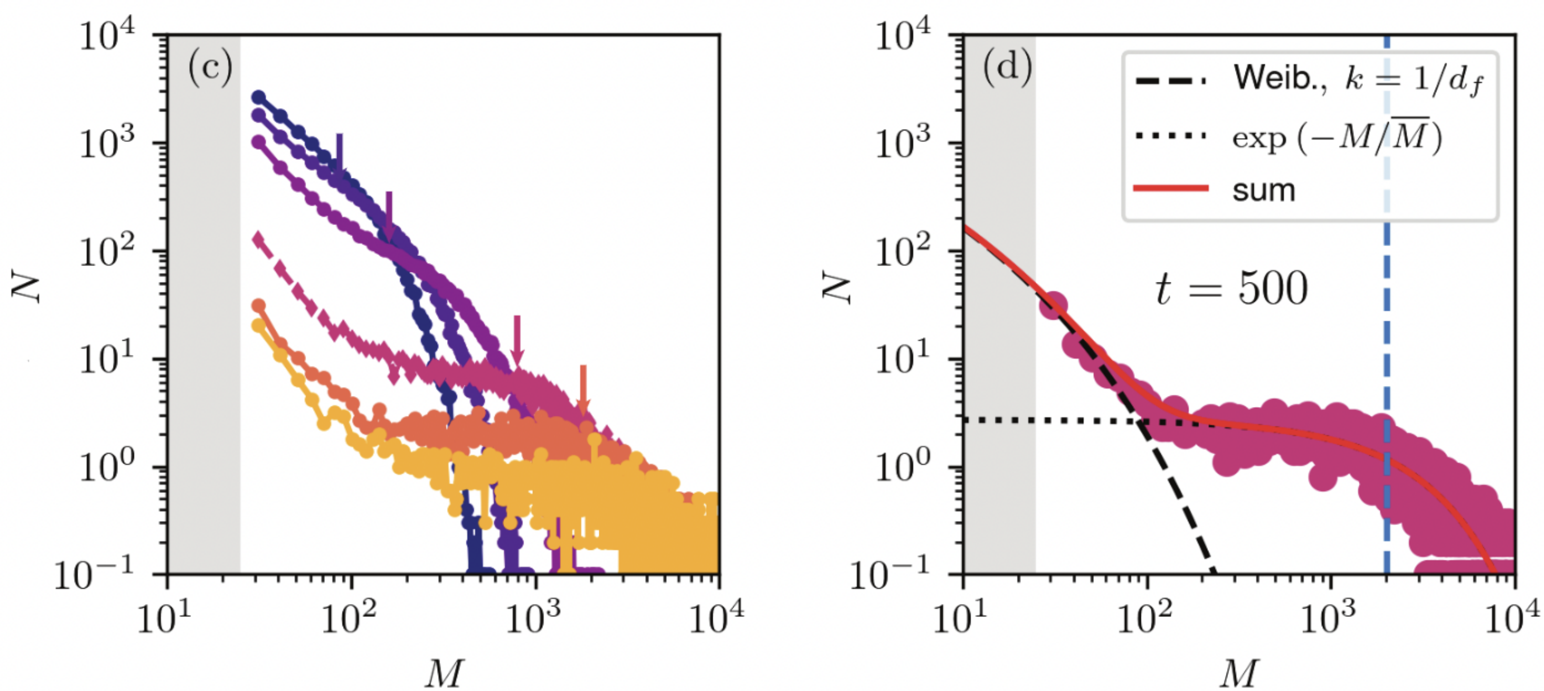

The arrows are at the average

Cluster-cluster aggregation

Extended Smoluchowski argument

$$[a] + [b] \xrightarrow{K_{ab}} [a+b]$$

$[a]$ ensemble of aggregates with mass m_a

$$\frac{\mathrm{d}n_c}{\mathrm{d}t} = \underbrace{\frac{1}{2}\sum_{a+b=c} K_{ab} n_a n_b}_{\text{gain}} - \underbrace{\sum_a K_{ac} n_a n_c}_{\text{loss}}$$

n_a number of $[a]$ clusters and $\sum_a n_a = N_c$ the total number of clusters

$d = 2$ **Brownian diffusion** $K_{ab} \propto D_a + D_b \sim m_a^{-\alpha} + m_b^{-\alpha}$

$D_a \sim m_a^{-\alpha}$ the diffusion constant **Homogeneity** $K_{\lambda a\, \lambda b} = \lambda^{-\alpha} K_{ab}$

Cluster-cluster aggregation

Extended Smoluchowski argument

From $\overline{R}_g \sim t^{1/z}$ and using $D(M) \sim M^{-\alpha}$

Smoluchowski eq. $\Rightarrow z = d_f(1+\alpha) - (d - d_w)$

Regular clusters $M < \overline{M}$

$d_f = d = d_w = 2$

$\alpha = 0.5$

$z = 2(1+0.5) = 3$

Fractal clusters $M > \overline{M}$

$d_f = 1.45, d = 2$ and $d_w \sim 2$

if, instead, $\boxed{\alpha = 1}$

$z = 1.45(1+1) \sim 3$

Reviews on the application of fractals to colloidal aggregation

R. Jullien, Croatia Chemica Acta 65, 215 (1992) P. Meakin, Physica Scripta 46, 295 (1992)